

# Changes in mitochondrial membrane potential during staurosporine-induced apoptosis in Jurkat cells

Jared L. Scarlett<sup>a</sup>, Philip W. Sheard<sup>b</sup>, Gillian Hughes<sup>a</sup>, Elizabeth C. Ledgerwood<sup>a</sup>, Hung-Hai Ku<sup>c</sup>, Michael P. Murphy<sup>a,\*</sup>

<sup>a</sup>Department of Biochemistry, University of Otago, P.O. Box 56, Dunedin, New Zealand

<sup>b</sup>Department of Physiology, University of Otago, P.O. Box 56, Dunedin, New Zealand

<sup>c</sup>Department of Anatomy, National Yang Ming University, Taipei, Taiwan

Received 22 May 2000

Edited by Vladimir Skulachev

**Abstract** Cytochrome *c* release from mitochondria is central to apoptosis, but the events leading up to it are disputed. The mitochondrial membrane potential has been reported to decrease, increase or remain unchanged during cytochrome *c* release. We measured mitochondrial membrane potential in Jurkat cells undergoing apoptosis by the uptake of the radiolabelled lipophilic cation TPMP, enabling small changes in potential to be determined. The ATP/ADP ratio, mitochondrial and cell volumes, plasma membrane potential and the mitochondrial membrane potential in permeabilised cells were also measured. Before cytochrome *c* release the mitochondrial membrane potential increased, followed by a decrease in potential associated with mitochondrial swelling and the release of cytochrome *c* and DDP-1, an intermembrane space house keeping protein. Mitochondrial swelling and cytochrome *c* release were both blocked by bongkreikic acid, an inhibitor of the permeability transition. We conclude that during apoptosis mitochondria undergo an initial priming phase associated with hyperpolarisation which leads to an effector phase, during which mitochondria swell and release cytochrome *c*. © 2000 Federation of European Biochemical Societies. Published by Elsevier Science B.V. All rights reserved.

**Key words:** Apoptosis; Mitochondrion; Membrane potential

## 1. Introduction

A number of pro- and anti-apoptotic members of the Bcl-2 protein family regulate the release of cytochrome *c* and apoptosis inducing factor (AIF) from the mitochondrial intermembrane space into the cytosol [1–7]. Cytochrome *c* then interacts with pro-caspase 9 and Apaf-1 to activate caspase 9 and thus switch on caspase 3 and commit the cell to apoptosis, in contrast AIF goes directly to the nucleus where it induces nuclear condensation [5–10]. There are considerable uncertainties about how cytochrome *c* and AIF are released from mitochondria and about the events leading up to their appearance in the cytosol. At least three scenarios have been pro-

posed: the pro-apoptotic proteins Bax and Bak accelerate opening of the voltage-dependent anion channel (VDAC) in the outer membrane and thereby specifically release cytochrome *c* [11,12]; apoptosis follows induction of the mitochondrial permeability transition, caused by formation of a pore in the inner membrane [13] which leads to matrix swelling, rupture of the outer membrane and release of AIF and cytochrome *c* [14–18]; finally, mitochondrial hyperpolarisation leads to swelling and outer membrane rupture, but without the mitochondrial depolarisation associated with the permeability transition [19,20].

The most informative measure of the changes associated with cytochrome *c* release is the mitochondrial membrane potential. However, such measurements in apoptotic cells have produced conflicting results, with reports of no decrease in potential until after cytochrome *c* release [21–25], a decrease in membrane potential associated with cytochrome *c* release [6,14–17,26], and finally an initial increase in potential followed by cytochrome *c* release without loss of membrane potential [19,20]. These measurements rely on the uptake of fluorescent dyes, which gives a qualitative indication of the membrane potential but can be difficult to quantitate and often fails to detect large changes in potential due to saturation of dye uptake [1,27–29]. Alterations to mitochondrial and cell volume and plasma membrane potential also contribute to dye uptake and must be taken into account before a change in mitochondrial potential is confirmed [27,30].

To overcome these difficulties we measured mitochondrial membrane potential changes during apoptosis using the uptake of the radiolabelled lipophilic cation methyltriphenylphosphonium (TPMP) [27,29–33]. The uptake of TPMP is easily quantitated and responds to the mitochondrial membrane potential over all values [27,30,33], enabling small changes in membrane potential to be measured sequentially at short time intervals during apoptosis. The Jurkat T lymphocyte cell line was chosen because it undergoes apoptosis by cytochrome *c* release in response to the protein kinase inhibitor staurosporine (STS). In parallel we measured the release into the cytosol of cytochrome *c* and an intermembrane space house keeping protein DDP-1, ATP/ADP ratio, mitochondrial swelling by stereological analysis of electron micrographs, caspase 3 activation, cell volume and plasma membrane potential. From these measurements we could correlate and order the events occurring during apoptosis. The mitochondrial membrane potential increased within 20 min of STS addition, followed about 40 min later by a gradual mitochondrial depolarisation associated with swelling, outer membrane

\*Corresponding author. Fax: (64)-3-479 7866.  
E-mail: [murphy@sanger.otago.ac.nz](mailto:murphy@sanger.otago.ac.nz)

**Abbreviations:** AIF, apoptosis inducing factor; AMC, aminomethylcoumarin; DDP-1, deafness dystonia peptide-1; FCCP, carbonyl cyanide-*p*-(trifluoromethoxy)phenylhydrazone; FCS, foetal calf serum; STS, staurosporine; TPB, sodium tetraphenylboron; TPMP, methyltriphenylphosphonium; VDAC, voltage-dependent anion channel

rupture and the release of cytochrome *c* and DDP-1 into the cytosol. This second phase of mitochondrial outer membrane rupture was blocked by bongkreikic acid, an inhibitor of the mitochondrial permeability transition. We conclude that mitochondria undergo two distinct phases during apoptosis: an initial priming phase that involves hyperpolarisation, which leads on to an effector phase involving depolarisation, swelling and cytochrome *c* release.

## 2. Materials and methods

### 2.1. Cell culture and incubations

The Jurkat human T lymphocyte cell line was grown in RPMI 1640 with 10% foetal calf serum (FCS), 100 U/ml penicillin, and 100 µg/ml streptomycin at 37°C in humidified air/5% CO<sub>2</sub>. Cells (2.5 × 10<sup>6</sup> ml) were incubated in 1 ml RPMI 1640 supplemented with 25 mM HEPES–NaOH (pH 7.4) and 1% FCS at 37°C and apoptosis induced with 2.5 µM STS. To measure the release of mitochondrial inter membrane space proteins into the cytosol, cells (5 × 10<sup>6</sup>) were pelleted and homogenised in 1 ml STE [250 mM sucrose, 5 mM Tris–HCl (pH 7.4) and 1 mM EGTA] containing Boehringer Mannheim Complete<sup>™</sup> protease inhibitors and the cytosolic fraction isolated by centrifugation (100 000 × *g* for 10 min in a Beckman Airfuge).

### 2.2. Apoptosis assays

To measure caspase 3 activity cells (2.5 × 10<sup>6</sup>) were pelleted by centrifugation, and suspended in 100 mM HEPES, 10% sucrose, 5 mM dithiothreitol, 10<sup>−6</sup> M NP-40 and 0.1% CHAPS at pH 7.25 supplemented with 50 µM DEVD-AMC. The release of AMC was measured in a Perkin-Elmer MPF-3L fluorescence spectrophotometer (excitation 355 nm, emission 460 nm) at 37°C, calibrated using an AMC standard curve. DNA was extracted from cells (2.5 × 10<sup>6</sup>) using a Qiagen DNeasy<sup>™</sup> tissue kit, and equal amounts separated by electrophoresis on a 2% agarose gel and visualised by ethidium bromide fluorescence. Annexin V binding was determined by incubating cells with Annexin V-Fluos (Roche) according to the manufacturer's instructions and Annexin positive cells were quantitated using a FACScan flow cytometer.

### 2.3. Immunoblotting

Proteins separated on a 15 or 17.5% Tris/Tricine gel, were transferred to nitrocellulose, incubated with primary antibody followed by horseradish peroxidase-conjugated secondary antibody and immunoreactivity was detected using the Pierce SuperSignal West Pico chemiluminescent substrate. Bands were quantitated using a Bio-Rad GS-670 imaging densitometer. The primary antibodies used were anti-pigeon cytochrome *c* monoclonal mouse IgG2b from Pharmingen and the anti-DDP-1 rabbit anti-serum raised against a GST-human DDP-1 fusion protein (kindly provided by Dr Carla Koehler, UCLA).

### 2.4. Measurement of mitochondrial membrane potential

Cells (2.5 × 10<sup>6</sup>) were incubated at 37°C in 1 ml RPMI/HEPES/FCS supplemented with 1 µM TPMP, 100 nCi/ml [<sup>3</sup>H]TPMP and 500 nM sodium tetraphenylboron (TPB). The total time of exposure to TPMP/TPB was always 60 min, consequently for longer incubations TPMP/TPB were added 60 min before the end of the incubation, while for shorter incubations TPMP/TPB were preincubated with cells before addition of STS. The lipophilic anion TPB facilitates rapid equilibration of TPMP [31,32]. After incubation the cells were pelleted by centrifugation (10 000 × *g* for 30 s), 50 µl supernatant removed, the cell pellet resuspended in 50 µl 20% Triton X-100 and the radioactivity in the pellet and supernatant quantitated using an LKB Wallac RackBeta liquid scintillation counter with appropriate quench corrections [31,32]. Non-specific TPMP binding to de-energised cells was determined in a parallel incubation supplemented with 12.5 µM oligomycin, 20 µM carbonyl cyanide-*p*-(trifluoromethoxy)phenylhydrazone (FCCP), 1 µM myxothiazol, 100 nM valinomycin, and 1 mM ouabain to eliminate mitochondrial and plasma membrane potentials. Energisation-dependent TPMP uptake is expressed as an accumulation ratio in units of [(TPMP/mg protein)/(TPMP/µl supernatant)] [32]. To measure TPMP accumulation by digitonin-permeabilised cells, cells were incubated as above, then pelleted and resuspended in 250 µl medium [120 mM KCl, 10 mM HEPES–KOH (pH 7.4)

and 1 mM EGTA] supplemented with 1 µM TPMP, 100 nCi/ml [<sup>3</sup>H]TPMP, 20 µg/ml digitonin, 10 mM succinate and 50 µM rotenone [34]. After 10 min at 37°C the permeabilised cells were pelleted by centrifugation (10 000 × *g* for 30 s), and the pellets and supernatants processed and assayed for radioactivity as above. Non-specific TPMP-binding was determined from parallel incubations supplemented with 400 nM FCCP and the energisation-dependent TPMP uptake was expressed as an accumulation ratio as above.

### 2.5. Transmission electron microscopy

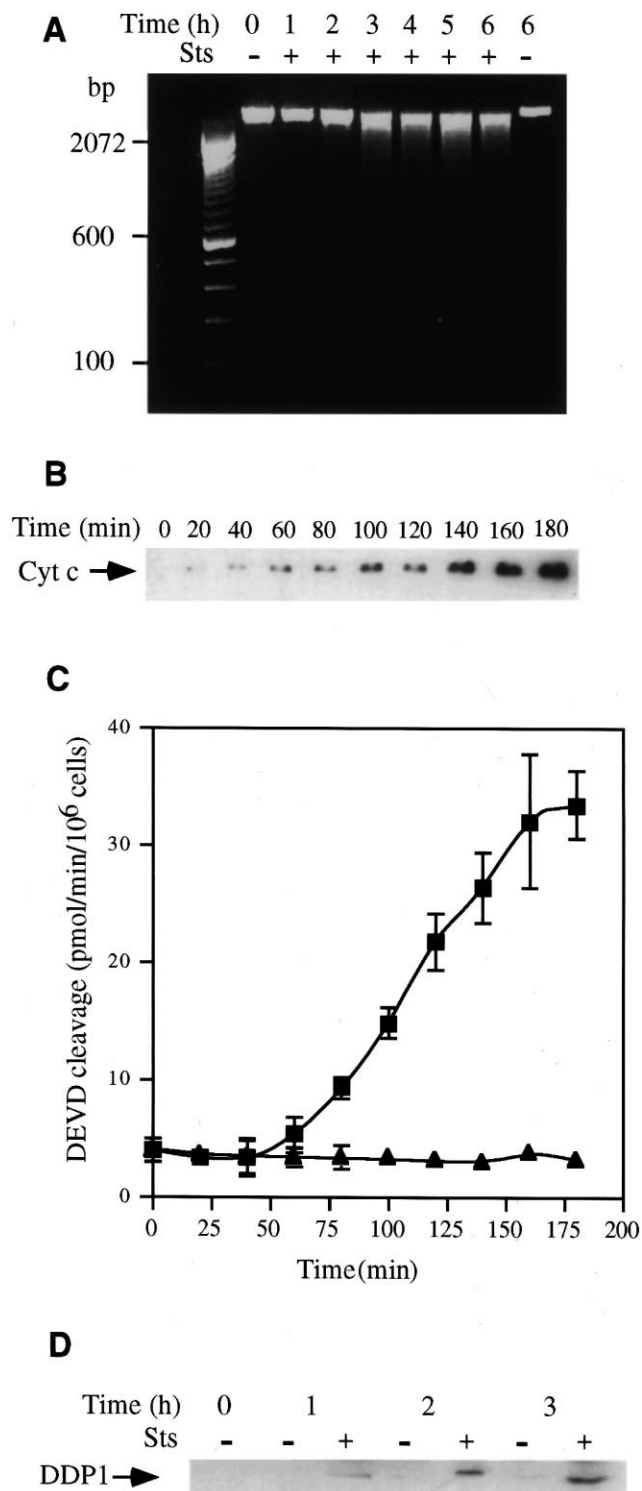
After incubation cells were pelleted by centrifugation (1000 × *g* for 2 min) placed in fixative (1% glutaraldehyde, 3 mM CaCl<sub>2</sub>, and 0.1 M cacodylate pH 7.2 in PBS) for 30 s, and then incubated in fresh fixative for 1 h at 37°C. The cell pellet was washed with 3 mM CaCl<sub>2</sub>, 0.15 M cacodylate, pH 7.2, warmed to 40°C and mixed with 2% (w/v) low melting point agarose in 0.1 M cacodylate (pH 7.2) and concentrated by centrifugation (1000 × *g* for 10 s). The agarose plugs were post-fixed in 1% OsO<sub>4</sub>, 1.5% potassium ferrocyanide and 100 mM cacodylate buffer for 60 min at room temperature, embedded in resin, and ultra thin sections were obtained for examination in a Philips 410 transmission electron microscope. The fraction of cytosol occupied by mitochondria was measured stereologically by overlaying 20 × 25 cm electron micrographs (19 000 × enlargements; 20 randomly selected for each determination) with a 15 mm square grid and counting grid points that intersect with either mitochondria or cytosol [32].

### 2.6. Other procedures

Protein concentrations were determined using the bicinchoninic acid assay with BSA as a standard [35]. The cellular ATP/ADP ratio was measured by quenching cell incubations in perchloric acid and assaying neutralised aliquots for ATP and ADP by a luciferase luminometer assay [34]. Plasma membrane potential was measured using standard intracellular recording techniques [34]. Cells were incubated as described above and then added to a glass petri dish, causing cells to stick to the substrate. Intracellular recordings were made with glass micropipettes filled with 3 M KCl. Pipettes typically had DC resistances of 40–60 MΩ. Membrane potentials were monitored with a WP Instruments (Sarasota, FL, USA) Cyto 721 electrometer amplifier, and the output was displayed using a MacLab system (AD Instruments, Castle Hill, Australia). For recording purposes, cells were maintained at ~24–26°C and data are means ± S.E.M. of 5–9 determinations on two or three separate cell incubations from cells that gave stable potential readings, indicating a good seal of the plasma membrane with the recording electrode. The potentials measured are the same as those determined for thymocytes from the equilibration of radiolabelled probes [30], indicating that after electrode insertion the plasma membrane potential immediately reestablished its normal value. Cell volume was measured from the exclusion of <sup>14</sup>C-inulin relative to <sup>3</sup>H<sub>2</sub>O [30,32].

## 3. Results

To determine the time scale of apoptosis, Jurkat cells were incubated with STS and DNA was extracted at hourly intervals (Fig. 1A). DNA laddering was detected within 3 h and was not seen in control incubations of up to 6 h (Fig. 1A). The proportion of Annexin positive cells was unchanged after incubation with STS for an hour, but increased to ~45% after 2 h incubation and to ~70% after 3 h incubation with STS. Nuclear condensation was also evident in electron micrographs of STS-treated cells after 3 h (data not shown). To confirm that apoptosis was a consequence of cytochrome *c* release from mitochondria and subsequent caspase activation we measured these at 20 min intervals over the 3 h leading up to DNA laddering (Fig. 1B,C). After 60–120 min increasing amounts of cytochrome *c* were detected in the cytoplasm with most release occurring from 120 to 180 min (Fig. 1B). Caspase 3 activity was negligible for up to 60 min, but from then on there was a steady increase in activity which peaked after 180 min (Fig. 1C). The activation of caspase 3 correlates



with cytochrome *c* release and precedes DNA laddering (Fig. 1). This sequence was confirmed by blocking caspase 3 activation, but not cytochrome *c* release, by the broad spectrum caspase inhibitor benzyloxycarbonyl-valinyl-alaninyl-aspartyl-(*O*-methyl)-fluoromethylketone (*z*-VAD-fmk) (data not shown). Deafness Dystonia Peptide 1 (DDP-1), a component of the mitochondrial protein import machinery in the inter-membrane space [36], was also released into the cytosol over the same time scale as cytochrome *c* (Fig. 1D).

Fig. 1. STS-induced apoptosis in Jurkat cells. Cells were incubated with 2.5  $\mu$ M STS for the indicated times. A: DNA was extracted from  $2.5 \times 10^6$  cells and separated on a 2% agarose gel and compared with a 100 bp ladder (left lane). B: Cytosolic fractions were analysed by immunoblotting for cytochrome *c*. C: caspase 3 activity was measured as the rate of DEVD-AMC cleavage in extracts from control (triangles) or STS-treated cells (squares). D: Cytosolic fractions were analysed by immunoblotting for DDP-1. Results are representative (A, B and D) or the means  $\pm$  S.E.M. (C) of at least three separate experiments.

To investigate the mitochondrial changes that precede and accompany cytochrome *c* release we measured the membrane potential at 20 min intervals during apoptosis from the accumulation of the radioactive lipophilic cation TPMP (Fig. 2A). The TPMP accumulation ratio increased within 20 min of STS treatment and remained elevated for about an hour. After this it steadily declined until there was no energy dependent TPMP accumulation after 3 h. In control cells there was no change in TPMP accumulation over 3 h. The initial elevation in TPMP accumulation was the same size as that caused by bongkreikic acid, an inhibitor of mitochondrial ATP transport. Changes in the cell volume and the plasma membrane potential affect TPMP accumulation by whole cells [30]. The cell volume was unchanged when measured 30 min after addition of STS or bongkreikic acid (control =  $0.2 \pm 0.06$  pl; +STS =  $0.16 \pm 0.06$  pl; +bongkreikic acid =  $0.17 \pm 0.05$  pl). The plasma membrane potentials of cells measured 20–40 min after addition of STS or bongkreikic acid were also unchanged (control =  $-38.3 \pm 8.4$  mV; +STS =  $-40.6 \pm 4.1$  mV; +bongkreikic acid =  $-41.0 \pm 2.9$  mV). Therefore the changes in TPMP accumulation by whole cells are due to mitochondria alone.

To determine whether these changes in mitochondrial membrane potential were due to permanent changes in the mitochondria themselves we incubated cells with STS, then we permeabilised the plasma membrane with digitonin and measured the TPMP accumulation ratio in the presence of a respiratory substrate. This procedure enables mitochondrial function to be analysed directly, without interference from non-mitochondrial factors, such as ATP-turnover and the plasma membrane potential [32]. STS treatment did not affect the TPMP accumulation ratios of permeabilised cells for up to 40 min, after which time the mitochondrial membrane potential steadily declined, indicating that the decrease in TPMP accumulation ratio seen after an hour in intact cells corresponds to irreversible disruption of the mitochondria (Fig. 2B). However, the initial hyperpolarisation seen in intact cells was not found in the permeabilised cells. As the mitochondria in the permeabilised cells are respiring in the absence of ATP turnover their membrane potential is at its maximum value, in contrast to the situation within cells where ATP synthesis keeps the mitochondrial membrane potential at a sub-maximal value. Therefore the increase in TPMP accumulation seen in intact cells is not due to a stable stimulation of the respiratory chain, but is more likely due to an inhibition of ATP synthesis leading to an increase in the mitochondrial membrane potential.

The cellular ATP/ADP ratio was determined as a further measure of changes in mitochondrial function during apoptosis (Fig. 2C). STS-treated cells maintained their ATP/ADP ratio for about 40 min, after which time the ratio steadily

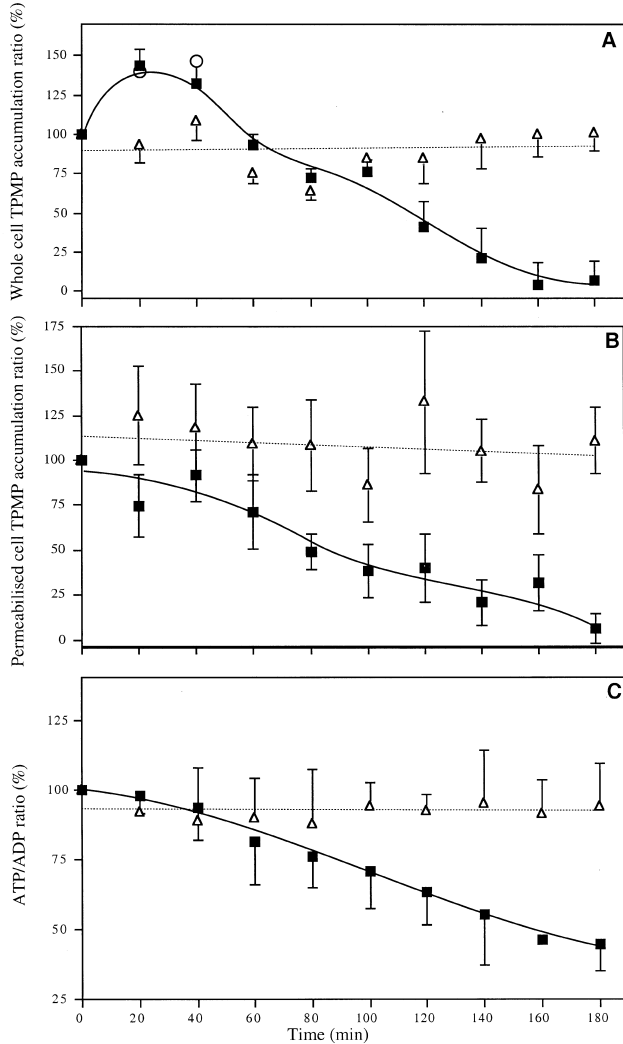


Fig. 2. Mitochondrial changes during apoptosis. Cells were incubated in the presence (filled squares) or absence (open triangles) of 2.5  $\mu$ M STS, or in the presence of 15  $\mu$ M bongkreikic acid (open circles). Measurements are expressed as a percentage of control incubations at time zero. A: Mitochondrial membrane potential in intact cells measured as a TPMP accumulation ratio. B: Intact cells were incubated with STS for the indicated times, then isolated, permeabilised with digitonin and their TPMP accumulation ratios determined. C: ATP/ADP ratio in intact cells. The ATP/ADP ratio of intact cells at time zero was about 10. All data are means  $\pm$  S.E.M. of at least three separate experiments.

declined, in parallel with the decrease in TPMP accumulation by intact and permeabilised cells.

To determine if the release of cytochrome *c* and DDP-1 from mitochondria seen in Fig. 1 was due to mitochondrial swelling and consequent outer membrane rupture, we visualised mitochondria within cells undergoing apoptosis by transmission electron microscopy (Fig. 3). No significant alterations in mitochondrial morphology were seen after 30 min of STS treatment (Fig. 3A,B). After 60 min mitochondria started to swell (Fig. 3C) and at 120 min (Fig. 3D) and particularly at 180 min (Fig. 3E), large swollen mitochondria could be seen. In contrast, the mitochondria in control cells were unchanged after 180 min (Fig. 3F). To quantitate swelling the mitochondrial volume was determined by stereological analysis of electron micrographs (Fig. 3G). There was no in-

crease in mitochondrial volume within 40 min of STS treatment, but swelling was evident at 60 min and peaked after 120 min (Fig. 3G), while the mitochondrial volume in control cells did not change (Fig. 3G). The lack of mitochondrial swelling within 40 min of STS treatment indicates that the

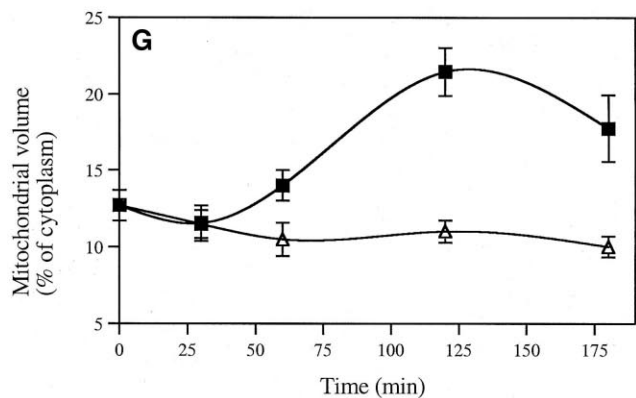
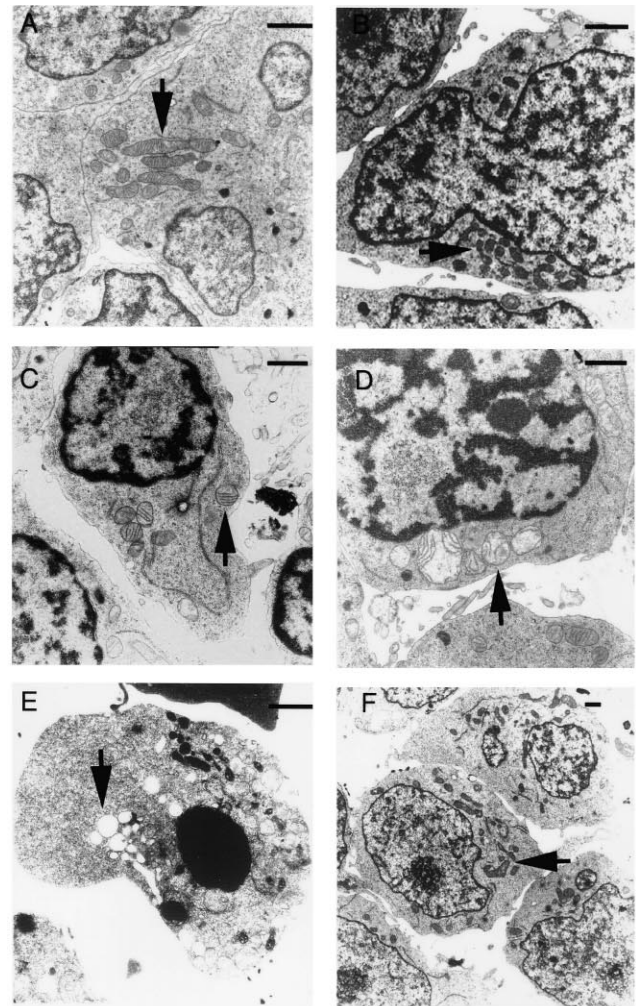


Fig. 3. Mitochondrial swelling during apoptosis. Cells were incubated in the presence or absence of STS, then fixed and examined by transmission electron microscopy. Control incubations were for 0 h (A) or 3 h (F). Incubations with STS were for 30 min (B), 1 h (C), 2 h (D) or 3 h (E). G: The mitochondrial volume in STS-treated (filled squares) or control cells (open triangles), determined by stereological analysis of 20 electron micrographs  $\pm$  S.E.M., for each time point.

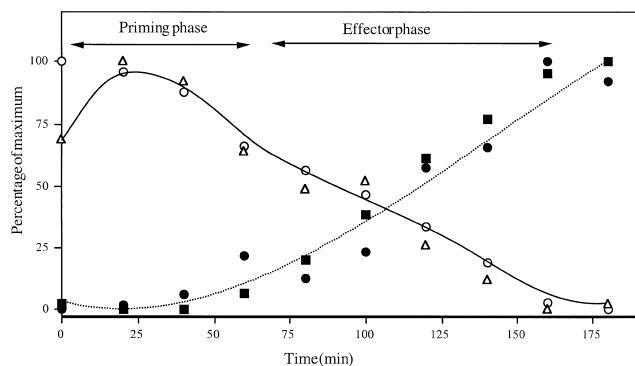


Fig. 4. The priming and effector phases of apoptosis. Changes in mitochondrial membrane potential (open triangles), ATP/ADP ratio (open circles), cytochrome *c* release (closed circles) and caspase activity (closed squares) are plotted against time. Data are normalised to show changes as a percentage of the difference between minimum and maximum values. The cytochrome *c* release data were obtained by scanning densitometry of three immunoblots similar to Fig. 1B.

early increase in TPMP accumulation by intact cells (Fig. 2A) was caused by an increase in membrane potential, rather than mitochondrial swelling.

To correlate the events occurring during apoptosis we plotted the normalised changes in membrane potential, ATP/ADP ratio, mitochondrial volume, cytochrome *c* release and caspase activation on a single graph (Fig. 4). This makes clear that there are two phases in the activation of apoptosis by mitochondria: a priming phase characterised by mitochondrial hyperpolarisation that occurs without swelling, release of cytochrome *c* or caspase activation. After about an hour this leads onto an effector phase during which there is a decline in membrane potential and ATP/ADP ratio associated with mitochondrial swelling, cytochrome *c* release and caspase activation (Fig. 4).

The mitochondrial changes seen during the effector phase of apoptosis have a number of similarities to induction of the mitochondrial permeability transition [13]. The permeability transition occurs following formation of a pore in the inner membrane that leads to depolarisation, swelling and rupture of the outer membrane, followed by the release of intermembrane space proteins [13,18]. Pre-incubating cells with the permeability transition inhibitor bongkrekic acid [16] prior to addition of STS blocked cytochrome *c* release, caspase 3 activation and mitochondrial swelling on addition of STS (data not shown).

#### 4. Discussion

Jurkat cells treated with the protein kinase inhibitor STS rapidly underwent apoptosis, with DNA degradation, Annexin V binding and nuclear condensation evident within 3 h (Fig. 1). Caspase activation, following cytochrome *c* release into the cytosol, preceded the nuclear changes and was detectable after an hour (Fig. 1). Our data enable us to draw conclusions about the events that occur in mitochondria in the hour leading up to cytochrome *c* release (the priming phase), and about how mitochondria then release cytochrome *c* (the effector phase).

The TPMP accumulation ratio of intact cells increased within 20 min and remained elevated for up to an hour during the priming phase (Fig. 2A). It was due to an increase in the

mitochondrial membrane potential itself, as there was no change in plasma membrane potential, or in cell or mitochondrial volume. An increase in activity of the respiratory chain was not responsible, as the membrane potential of mitochondria in digitonin-permeabilised cells in state 4 was unchanged over the first hour (Fig. 2B). This finding of an increase in membrane potential early in apoptosis is in agreement with other reports [19,20,37]. Inhibition of mitochondrial ATP transport by bongkrekic acid increased TPMP accumulation to the same extent as STS (Fig. 2A) by shifting the cells from state 3, where ATP synthesis decreases the potential, to state 4 where the absence of ATP synthesis leads to maximal potential. STS could also do this by inhibiting either ATP synthesis or transport, but inhibition of transport is the likely cause as this is known to decrease in cells undergoing apoptosis [20]. The decrease in ATP transport could arise from impeding the adenine nucleotide carrier in the inner membrane and/or VDAC in the outer membrane. As both proteins are components of the permeability transition pore a link between inhibition of ATP transport and induction of the permeability transition is suggested.

The release of cytochrome *c* from the intermembrane space into the cytosol was associated with mitochondrial swelling and the release of other intermembrane space proteins (Figs. 1,3 and 4). This suggests that swelling and outer membrane rupture is the mechanism of release (Fig. 1), and this is supported by other reports of the release of house keeping intermembrane space proteins [24] and mitochondrial swelling [19] during apoptosis. This swelling correlates with a decline in membrane potential and ATP/ADP ratio in intact cells, and also with a decrease in the membrane potential in permeabilised cells (Fig. 2). That cytochrome *c* release occurs at the same time as an irreversible decline in mitochondrial function and is associated with swelling and permeabilisation of the outer membrane is consistent with induction of the mitochondrial permeability transition [18]. Supporting this, the permeability transition inhibitor bongkrekic acid prevented mitochondrial swelling and release of cytochrome *c*.

There was no release of cytochrome *c* without a decrease in mitochondrial membrane potential (Fig. 4). How can this be reconciled with the many reports that cytochrome *c* release occurs before a decrease in membrane potential [19,23–25]? While the decline in membrane potential started after an hour, by 2 h there was still a substantial potential present, even though considerable cytochrome *c* release had occurred (Fig. 4). This residual potential may be sufficient to cause substantial uptake of fluorescent dyes into mitochondria that is difficult to distinguish from that by fully energised mitochondria [29]. Alternatively, there is growing evidence for two pathways of cytochrome *c* release from mitochondria during apoptosis: rupture of the outer membrane following swelling, or through a specific pore in the outer membrane [1,11,12]. In liposomes and yeast Bax and Bak interact with VDAC to cause selective cytochrome *c* release [12]. Addition of recombinant Bax to isolated mitochondria induced cytochrome *c* loss without swelling [11], however others have shown that Bax does induce the permeability transition in isolated mitochondria and within cells [38,39]. However cleavage of Bid by caspase 8 leads to a Bid fragment that facilitates Bax insertion into the outer membrane and thereby induces cytochrome *c* release independently of the permeability transition [1,40]. In summary, the pro-apoptotic proteins Bax and Bak interact with

both VDAC and the adenine nucleotide carrier. In some circumstances this may lead to assembly of the permeability transition pore, mitochondrial swelling, outer membrane rupture and cytochrome *c* release. However under different conditions the interaction between Bax/Bak and VDAC may form an outer membrane pore selective for cytochrome *c*, but it is unclear if this occurs in mammalian cells undergoing apoptosis, or is an artifact of disruption of VDAC by Bax/Bak in heterologous and in vitro systems.

In conclusion, we have shown that there are two phases of mitochondrial activity during STS-induced apoptosis in Jurkat cells. An early priming phase associated with an increased membrane potential, followed by an effector phase associated with a decline in mitochondrial function, mitochondrial swelling and release of inter membrane space proteins into the cytosol. An appealing scenario to explain these data is that during the priming phase the adenine nucleotide carrier, VDAC, cyclophilin D and other proteins are recruited to form the permeability transition pore [13]. The depletion of functional adenine nucleotide carrier and/or VDAC decreases ATP transport, thus increasing the membrane potential due to the shift from state 3 to state 4. After 40 min or so, sufficient permeability transition pores have formed to decrease the membrane potential and initiate mitochondrial swelling and cytochrome *c* release. bongkreikic acid and anti-apoptotic proteins such as Bcl-X<sub>L</sub> may act by decreasing the availability of the adenine nucleotide carrier and/or VDAC to form permeability transition pores [19].

*Acknowledgements:* This work was supported by grants to M.P.M. from the Health Research Council of NZ, the Marsden Fund administered by the Royal Society of NZ and the Neurological Foundation of NZ. J.L.S. is a Miller Scholar of the Neurological Foundation of NZ.

## References

- [1] Green, D.R. and Reed, J.C. (1998) *Science* 281, 1309–1312.
- [2] Reed, J.C., Jurgensmeier, J. and Matsuyama, S. (1998) *Biochim. Biophys. Acta* 1366, 127–137.
- [3] Adams, J.M. and Cory, S. (1998) *Science* 281, 1322–1326.
- [4] Liu, X.S., Kim, C.N., Yang, J., Jemmerson, R. and Wang, X.D. (1996) *Cell* 86, 147–157.
- [5] Li, P., Nijhawan, I., Budihardjo, I., Srinivasula, S.M., Ahmad, M., Alnemri, E.S. and Wang, X. (1997) *Cell* 91, 479–489.
- [6] Susin, S.A., Lorenzo, H.K., Zamzami, N., Marzo, I., Snow, B.E., Brothers, G.M., Mangion, J., Jacotot, E., Costantini, P., Loeffler, M., Larochette, N., Goodlett, D.R., Aebersold, R., Siderovski, D.P., Penninger, J.M. and Kroemer, G. (1999) *Nature* 397, 441–446.
- [7] Susin, S.A., Zamzami, N., Castedo, M., Hirsch, T., Marchetti, P., Macho, A., Daugas, E., Geuskens, M. and Kroemer, G. (1996) *J. Exp. Med.* 184, 1–11.
- [8] Hu, Y., Benedict, M.A., Wu, D., Inohara, N. and Nunez, G. (1998) *Proc. Natl. Acad. Sci. USA* 95, 4386–4391.
- [9] Enari, M., Sakahira, H., Yokoyama, H., Okawa, K., Iwamatsu, A. and Nagata, S. (1998) *Nature* 391, 43–50.
- [10] Nicholson, D.W. and Thornberry, N.A. (1997) *Trends Biochem. Sci.* 22, 299–306.
- [11] Jurgensmeier, J.M., Xie, Z., Deveraux, Q., Ellerby, L., Bredesen, D. and Reed, J.C. (1998) *Proc. Natl. Acad. Sci. USA* 95, 4997–5002.
- [12] Shimizu, S., Narita, M. and Tsujimoto, Y. (1999) *Nature* 399, 483–487.
- [13] Zoratti, M. and Szabo, I. (1995) *Biochim. Biophys. Acta* 1241, 139–176.
- [14] Zamzami, N., Marchetti, P., Castedo, M., Zanin, C., Vayssières, J.L., Petit, P.X. and Kroemer, G. (1995) *J. Exp. Med.* 181, 1661–1672.
- [15] Zamzami, N., Marchetti, P., Castedo, M., Decaudin, D., Macho, A., Hirsch, T., Susin, S.A., Petit, P.X., Mignotte, B. and Kroemer, G. (1995) *J. Exp. Med.* 182, 367–377.
- [16] Zamzami, N., Marchetti, P., Castedo, M., Hirsch, T., Susin, S., Masse, B. and Kroemer, G. (1996) *FEBS Lett.* 384, 53–57.
- [17] Zamzami, N., Susin, S.A., Marchetti, P., Hirsch, T., Gomez-Monterrey, I., Castedo, M. and Kroemer, G. (1996) *J. Exp. Med.* 183, 1533–1544.
- [18] Scarlett, J.L. and Murphy, M.P. (1997) *FEBS Lett.* 418, 282–286.
- [19] Vander Heiden, M.G., Chandel, N.S., Williamson, E.K., Schumaker, P.T. and Thompson, C.B. (1997) *Cell* 91, 627–637.
- [20] Vander Heiden, M.G., Chandel, N.S., Schumacker, P.T. and Thompson, C.B. (1999) *Mol. Cell* 3, 159–167.
- [21] Bossy-Wetzel, E., Newmeyer, D.D. and Green, D.R. (1998) *EMBO J.* 17, 37–49.
- [22] Kluck, R.M., Bossy-Wetzel, E., Green, D.R. and Newmeyer, D.D. (1997) *Science* 275, 1132–1136.
- [23] Yang, J., Liu, X., Bhalla, K., Kim, C.N., Ibrado, A.M., Cai, J., Peng, T.-L., Jones, D.P. and Wang, X. (1997) *Science* 275, 1129–1132.
- [24] Samali, A., Cai, J., Zhivotovsky, B., Jones, D.P. and Orrenius, S. (1999) *EMBO J.* 18, 2040–2048.
- [25] Goldstein, J.C., Waterhouse, N.J., Juin, P., Evan, G.I. and Green, D.R. (2000) *Nat. Cell Biol.* 2, 156–162.
- [26] Heiskanen, K.M., Bha, M.B., Wang, H.-W., Ma, J. and Nieminen, A.-L. (1999) *J. Biol. Chem.* 274, 5654–5658.
- [27] Azzone, G.F., Pietrobon, D. and Zoratti, M. (1984) *Cur. Top. Bioenerget.* 13, 1–77.
- [28] Salvioi, S., Ardizzoni, A., Franceschi, C. and Cossarizza, A. (1997) *FEBS Lett.* 411, 77–82.
- [29] Appleby, R.D., Porteous, W.K., Hughes, G., James, A.M., Shannon, D., Wei, Y.-H. and Murphy, M.P. (1999) *Eur. J. Biochem.* 262, 108–116.
- [30] Brand, M.D. (1995) in: *Bioenergetics – a Practical Approach* (Brown, G.C. and Cooper, C.E., Eds.), pp. 39–62, IRL, Oxford.
- [31] James, A.J., Sheard, P.W., Wei, Y.-H. and Murphy, M.P. (1999) *Eur. J. Biochem.* 259, 462–469.
- [32] James, A.M., Wei, Y.-H., Pang, C.-Y. and Murphy, M.P. (1996) *Biochem. J.* 318, 401–407.
- [33] Griinius, L.L., Jasaitis, A.A., Kadziauskas, J.P., Liberman, E.A., Skulachev, V.P., Topali, V.P. and Vladimirova, M.A. (1970) *Biochim. Biophys. Acta* 216, 1–12.
- [34] Porteous, W.K., James, A.M., Sheard, P.W., Porteous, C.M., Packer, M.A., Hyslop, S.J., Melton, J.V., Pang, C.-Y., Wei, Y.-H. and Murphy, M.P. (1998) *Eur. J. Biochem.* 257, 192–201.
- [35] Smith, P.K., Krohn, R.I., Hermanson, G.T., Mallia, A.K., Gartner, F.H., Provenzano, M.D., Fujimoto, E.K., Goeke, N.M., Olson, B.J. and Klenk, D.C. (1985) *Anal. Biochem.* 150, 76–85.
- [36] Koehler, C.M., Leuenberger, D., Merchant, S., Renold, A., Junne, T. and Schatz, G. (1999) *Proc. Natl. Acad. Sci. USA* 96, 2141–2146.
- [37] Banki, K., Hutter, E., Gonchoroff, N.J. and Perl, A. (1999) *J. Immunol.* 162, 1466–1479.
- [38] Narita, M., Shimizu, S., Ito, T., Chittenden, T., Lutz, R.J., Matsuda, H. and Tsujimoto, Y. (1998) *Proc. Natl. Acad. Sci. USA* 95, 14681–14686.
- [39] Marzo, I., Brenner, C., Zamzami, N., Jurgensmeier, J.M., Susin, S.A., Vieira, H.L.A., Prevost, M.-C., Xie, Z., Matsuyama, S., Reed, J.C. and Kroemer, G. (1998) *Science* 281, 2027–2031.
- [40] Eskes, R., Desagher, S., Antonsson, B. and Martinou, J.-C. (2000) *Mol. Cell. Biol.* 20, 929–935.